Structural Performance of Cold-formed Lean Duplex Stainless Steel Beams at Elevated Temperatures

Structural Performance of Cold-formed Lean Duplex Stainless Steel Beams at Elevated Temperatures

Yuner Huang[1]* and Ben Young[2]

[1] *Institute for Infrastructure and Environment, School of Engineering, University of Edinburgh, UK*

[2] *Department of Civil Engineering, The University of Hong Kong, Pokfulam Road, Hong Kong, China*

ABSTRACT: The structural performance of cold-formed lean duplex stainless steel beams at elevated temperatures ranging from 24 – 900 ºC was investigated in this study. A finite element model was developed. The numerical analysis covered the specimens of square and rectangular hollow sections. The material properties obtained from tensile coupon tests on lean duplex stainless steel at elevated temperatures were used in the finite element model. A total of 125 numerical flexural strengths were obtained from the finite element analysis. The numerical results were compared with the design values calculated by the existing design rules, including the American Specification, Australian/New Zealand Standard, European Code, direct strength method and continuous strength method. The suitability of these design rules for lean duplex stainless steel beams at elevated temperatures was assessed using reliability analysis. It was shown that the existing design rules are generally quite conservative in predicting the flexural strengths at elevated temperatures, except that the modified direct strength method provides accurate and reliable predictions. Therefore, it is recommended that the modified direct strength method be used for cold-formed lean duplex stainless steel beams at elevated temperatures.

Keywords: Beam; cold-formed; elevated temperatures; lean duplex; stainless steel; structural design.

Corresponding author. Tel.: +44 (0) 131 650 5736; Fax: +44 (0) 131 650 6554.
E-mail address: Yuner.Huang@ed.ac.uk

1. Introduction

A relatively new type of cold-formed lean duplex stainless steel is becoming an attractive choice as a construction material. Lean duplex stainless steel is characterized by a low nickel content of around 1.5%. Thus, lean duplex stainless steel has economic advantages over the other types of stainless steel. In addition, it is regarded as a high strength material with the nominal yield strength (0.2% proof stress) of 450 MPa [1]. However, there has been limited research on the structural performance and design of lean duplex stainless steel members, especially at elevated temperatures. Therefore, research on the lean duplex stainless steel material and structural members is required.

Lean duplex stainless steel is a relative new construction material. The previous research on lean duplex stainless steel focused mainly on the material properties and design of structural members at room temperature. Huang and Young [2], as well as Theofanous and Gardner [3], conducted tensile coupon tests and stub column tests to investigate the mechanical and section properties of cold-formed lean duplex stainless steel rectangular and square hollow sections. Experimental and numerical investigations were carried out on cold-formed lean duplex stainless steel columns [3, 4, 5, 6], and the test and numerical data were compared with the predicted column strengths calculated by the existing design rules. It was shown that the existing design rules, including design rules in the European Code, explicit approach in the Australian/New Zealand Standard and the direct strength method, are quite conservative for the lean duplex stainless steel. The implicit approach for column design in the American Specification and Australian/New Zealand Standard provides accurate predictions, but the iterative calculation procedure is tedious. Therefore, modified design rules have been proposed for better prediction of lean duplex stainless steel structural strengths. Some research has also been conducted for cold-formed lean duplex stainless steel beams [7, 8, 9, 10]. This research indicated that the existing European Code and direct strength method are quite conservative for lean duplex stainless steel flexural members, while the continuous strength method provides a better prediction. The European Code and direct strength method were found to be suitable for the shear design of lean duplex stainless steel rectangular hollow beams. The existing design rules in the European Code and the Australian/New Zealand Standard are generally quite conservative for lean duplex stainless steel beam-column members [11, 12]. The mechanical properties of cold-formed lean duplex stainless steel at elevated temperatures have been

investigated in previous research [13, 14]. Huang and Young [13] conducted tensile coupon tests on lean duplex stainless steel in both steady and transient states. The existing design rules for predicting the reduced material properties at elevated temperatures were assessed for lean duplex stainless steel. A modified design rule was proposed for lean duplex stainless steel material properties at elevated temperatures. Gardner et al. [14] summarized the results of tests on material properties of various stainless steel alloys at elevated temperatures, including the lean duplex stainless steel material reported by Outokumpu [15]. Reduction factors of strength and stiffness for lean duplex stainless steel were proposed according to the available data.

A search of the literature revealed a lack of research on cold-formed lean duplex stainless steel beams at elevated temperatures. Therefore, the objective of this study was to investigate the structural performance of cold-formed lean duplex stainless steel beams at elevated temperatures, ranging from 24 – 900 ºC, using finite element analysis. The reduced mechanical properties at elevated temperatures were used in the FEM. A total number of 125 numerical flexural strengths were compared with the design values calculated from the existing design rules. The applicability of the existing design rules for the lean duplex stainless steel beams was assessed using reliability analysis. According to the comparison, recommendations for designing cold-formed lean duplex stainless steel flexural members at elevated temperatures are proposed based on this study.

2. Finite Element Model

The finite element model (FEM) for cold-formed lean duplex stainless steel flexural members was developed by Huang and Young [7] using the program ABAQUS version 6.11 [16]. The FEM has been verified with the test results of four-point bending tests at room temperature. The moment-curvature curves and the failure modes predicted by the FEM have been found to agree well with the test results. In this study, the FEM developed by Huang and Young [7] was used for the finite element analysis of flexural members at elevated temperatures, except that the materials properties at room temperature were replaced by the reduced material properties obtained from tensile coupon tests at elevated temperatures [13]. The mechanical properties of section 50×50×1.5 obtained from the tensile coupon tests at 24 ºC, 300 ºC, 500 ºC, 700 ºC and 900 ºC using the steady-state test method were used in the FEM. ABAQUS allows for a multi-linear stress-strain curve to be used. Similar to the Huang and Young FEM [7], the first part of

the curve represents the elastic part up to the proportional limit stress with the measured Young's modulus and Poisson's ratio taken as 0.3. In the plastic analysis, the static stress-strain curve obtained from tensile coupon tests was converted to true stress and logarithmic true plastic strain curve, as described by Huang and Young [7]. The material properties adopted in the FEM, including the modulus of elasticity, yield strength, and ultimate strength at high temperatures ranging from 24 – 900 °C, are summarized in Table 1. Similar to the FEM for beams at room temperature, the local imperfection of $t/10$ was incorporated into the FEM, where t is the thickness of the sections. The residual stresses in the sections were not included.

3. Parametric Study

A total of 125 cold-formed lean duplex stainless steel flexural members at elevated temperatures, ranging from 24 – 900 ºC, were investigated in the parametric study. The finite element model (FEM) in the parametric study was identical to the FEM developed by Huang and Young [7], except that the mechanical properties obtained from the tensile coupon tests at elevated temperatures were used. The parametric study included square hollow sections (SHS) and rectangular hollow sections (RHS), which had one SHS of 300×300 (overall depth × overall width) as well as four RHS of 100×50, 50×100, 300×100 and 100×300. Five different thicknesses were designed for each section, in order to cover a wide range of slenderness ratios, from stocky to slender sections. The length of moment span between the two loading points was equal to the length of shear spans between the loading points to the supports for the flexural members. The lengths were designed carefully so that the section flexural capacity could be reached without shear failure. The specimens with the same cross-sectional dimensions and specimen lengths were investigated under five different temperatures in the finite element analysis, including 24 ºC, 300 ºC, 500 ºC, 700 ºC and 900 ºC. The RHS specimens were subjected to both major and minor axes bending. The specimens in the parametric study were labelled such that the cross-section dimension, specimen length and the specimen temperature could be identified, as shown in Table 1. The numbers before the letter "L" defined the cross-sectional dimensions (D×B×t), the number between the letter "L" and letter "T" was the specimen length in millimeters, and the number after the letter "T" was the specimen temperature in degrees Celsius. For example, the label 100×50×5L900T300 defined the flexural member with cross-section (D×B×t) of 100×50×5 in millimeters, and the specimen length of 900 mm as well as the specimen temperature of 300 ºC. The dimension of the overall

web depth (D) was larger than the overall flange width (B), thus the beam was subjected to major axis bending. On the other hand, the specimen 50×100×5L900T300 had the same cross-sectional dimension and length, but was subjected to minor axis bending. The finite element model of specimen 50×100×2L900T700 in the parametric study is shown in Figure 1. The moment-curvature curves of sections 300×100×10L2100, 300×100×7L2100, 100×300×15L1500, 100×300×4L1500 at elevated temperatures obtained from FEA are shown in Figures 2 – 5, respectively. The moment capacity ($M_{FEA,T}$) and the corresponding curvature ($k_{FEA,T}$) obtained from the finite element analysis are summarized in Table 2.

4. Design Rules & Comparison with Beam Strengths

The existing and modified design rules for cold-formed lean duplex stainless steel flexural members at elevated temperatures were assessed by comparing the design values with the 125 FEA flexural strengths ($M_{FEA,T}$), as summarized in Table 3. The unfactored design strengths (nominal strength) were calculated using (1) American Specification (ASCE) [17] ($M_{yielding,T}$, $M_{inelastic,T}$), (2) Australian/New Zealand Standard (AS/NZS) [18] ($M_{yielding,T}$, $M_{inelastic,T}$), (3) modified ASCE and AS/NZS described in Huang and Young [7] ($M^{\#}_{inelastic,T}$), (4) European Code (EC3) [19] ($M_{EC3,T}$), (5) suggested EC3 by Gardner and Theofanous [20] ($M_{G\&T,T}$), (6) modified EC3 in Huang and Young [7] ($M^{\#}_{EC3,T}$), (7) direct strength method (DSM) in AISI [21] ($M_{DSM,T}$, $M^{\wedge}_{DSM,T}$), (8) modified DSM in Huang and Young [7] ($M^{\#}_{DSM,T}$), and (9) continuous strength method (CSM) described in Saliba and Gardner [9] ($M_{CSM,T}$). The reduced material properties at elevated temperature, which were obtained from the tensile coupon tests for section 50×50×1.5 at elevated temperatures [7], were used in the calculation of design strengths at elevated temperatures. The design rules in the (1) ASCE [17], (2) AS/NZS [18], (3) modified ASCE and AS/NZS in Huang and Young [7], (4) EC3 [19], (5) suggested EC3 by Gardner and Theofanous [20], and (6) modified EC3 in Huang and Young [7] use the effective width method for the sections when local buckling occurs. Therefore, the calculation procedure using these design rules involved an iterative process, as the location of the neutral axis shifts with the effective width when the sections subjected to bending. However, such a tedious iterative process is not required in the DSM and CSM, as the flexural strength is calculated by the full section instead of the effective section.

4.1 Reliability Analysis

The reliability of the existing design rules for cold-formed lean duplex stainless steel flexural members at elevated temperatures was evaluated using reliability analysis, which is detailed in the Commentary of the ASCE Specifications [17]. A target reliability index (β_0) of 2.5 for stainless steel structural members was used as the lower limit. The design rules are considered to be reliable if the reliability index is greater than or equal to 2.5. The resistance factors (ϕ_0) of 0.90 for members with stiffened compression flanges subjected to bending is recommended by ASCE [17], AS/NZS [18], and AISI Standard [21] for the direct strength method (DSM), while the resistance factors of 0.91 are used by the EC3 [19] and modified EC3 by Gardner and Theofanous [20] as well as the continuous strength method (CSM) [9]. The load combinations of 1.2DL+1.6LL, 1.2DL+1.5LL and 1.35DL+1.5LL were used for design rules in ASCE, AS/NZS and EC3 in the reliability analysis, respectively, where DL is the dead load and LL is the live load. The load combinations of 1.35DL+1.5LL were used for reliability analysis of the modified EC3 by Gardner and Theofanous [20] and continuous strength method (CSM) [9], while the load combination of 1.2DL+1.6LL was used for the direct strength method (DSM) [21]. The Eq. 6.2-2 in the ASCE Specification [17] was used in calculating the reliability index. The statistical parameters M_m = 1.10, F_m = 1.00, V_M = 0.10 and V_F = 0.05, which are the mean values and coefficients of variation for material properties and fabrication factors for flexural members in Clause 3.3.1.1 of the commentary of the ASCE Specification were adopted. The mean value (P_m) and coefficient of variation (V_P) of numerical-to-predicted load or moment ratio are shown in Table 3. In calculating the reliability index, Eq. K2.1.1-4 in the North American cold-formed steel Specification AISI S100 [21] was used to calculate the correction factor, in order to account for the influence of the number of data. For the purpose of direct comparison, a constant resistant factor (ϕ_1) of 0.90 and a load combination of 1.2DL+1.6LL were used to calculate the reliability index (β_1) for the design rules; the values of the reliability index are also shown in Table 3.

4.2 American Specification and Australian/New Zealand Standard

The design rules for calculating the moment capacity for flexural members in the ASCE [17] and AS/NZS [18] are same. Both of the specifications allow for calculations based on the initiation of yielding and inelastic reserve capacity. Therefore, both approaches were assessed in this study. For the initiation of yielding, the moment capacities ($M_{yielding,T}$) were calculated

by the effective section modulus (S_e) multiplied by the yield strength (f_y). The reduced material properties at elevated temperatures were used in the calculations. The effective width was calculated in accordance with Clause 2.2 of ASCE and AS/NZS, where yield strength at the extreme fibre of compressive flange and the stress distribution varying linearly in the section were assumed. The comparison of the numerical strengths with the design strengths of lean duplex stainless steel flexural members at elevated temperatures is shown in Table 3 and Figure 6. For the approach by initiation of yielding, the design rules were found to be quite conservative and scattered in predicting the moment capacities of cold-formed lean duplex stainless steel members at elevated temperatures. The mean value of the numerical strengths ($M_{FEA,T}$) to design values ($M_{yielding,T}$) ratio was 1.51 with a COV of 0.277. The reliability indices (β_0) were 2.80 and 2.65 for ASCE [17] and AS/NZS [18], respectively.

For the approach by inelastic reserve capacity, the moment capacities ($M_{inelastic,T}$) were calculated by the equivalent force multiplying the lever arm within the section, considering equilibrium of the stresses in the effective section and assuming an ideally elastic-plastic stress distribution in the section. The compression strain factor (C_y) was calculated to determine the stress distribution in the section. However, the ASCE (2002) and AS/NZS (2001) did not state clearly the calculation of effective widths that involved elastic-plastic stress distribution in the section, and the calculation procedures for the effective width used in this study were the same as those detailed in Huang and Young [7]. The inelastic reserve capacity approach was less conservative than the initiation of yielding for lean duplex stainless steel flexural members at elevated temperatures, as shown in Table 3 and Figure 6. The mean value of numerical-to-design strengths ratio $M_{FEA,T}/M_{inelastic,T}$ was equal to 1.30 with a COV of 0.213. The reliability indices (β_0) were 2.74 and 2.57 for ASCE and AS/NZS, respectively.

The design rules based on the inelastic reserve capacity were modified to provide more accurate and reliable predictions for the lean duplex stainless steel flexural members at room temperature by Huang and Young [7]. The modification for the design rules consisted of three parts, namely for (i) effective width calculation; (ii) upper bound limit of moment capacity; and (iii) limitation of web slenderness (d_w/t ratio), as detailed in Huang and Young [7]. The suitability of modified design rules for lean duplex stainless steel flexural members at elevated temperatures was also assessed. The moment capacities ($M^{\#}_{inelastic,T}$) calculated by the modified design rule were compared with the numerical moment capacities ($M_{FEA,T}$) at elevated

temperatures, as shown in Table 3 and Figure 6. The modified design rules provided better predictions than the existing design rules. The mean value of $M_{FEA,T}/M^{\#}_{inelastic,T}$ was 1.16 with a COV of 0.105. The reliability index (β_0) was 2.97 for ASCE [17], while that for AS/NZS [18] was 2.75, both of which were greater than the target value.

4.3 European Code

The moment capacity ($M_{EC3,T}$) at elevated temperatures was calculated by European Code Part 1.4 [20]. The reduced material properties at elevated temperatures were used in the calculation. Classification for the sections and calculation of effective widths are required in EC3. The comparison of the numerical moment capacity ($M_{FEA,T}$) with the design values ($M_{EC3,T}$) at elevated temperatures are shown in Table 3 and Figure 7. It is found that the design rules provided less conservative and less scattered predictions for the lean duplex stainless steel flexural members at elevated temperatures compared with those at room temperature [7]. The mean value of M_u/M_{EC3} at room temperature was equal to 1.25 with the corresponding COV of 0.147, as shown in Huang and Young [7]; while the mean value of $M_{FEA,T}/M_{EC3,T}$ at elevated temperatures were equal to 1.19 with COV of 0.112. The reliability index (β_0) for $M_{FEA,T}/M_{EC3,T}$ at elevated temperatures was 2.82, which was greater than the target value of 2.5.

The classification limits and the effective width calculation in the European Code [19] for stainless steel were assessed by Gardner and Theofanous [20]. A set of classification limits for compression elements was proposed, and the effective width equations were modified [20]. It was shown by Huang and Young [7] that the suggested method by Gardner and Theofanous [20] provides a more accurate and less scattered prediction for lean duplex stainless steel flexural members at room temperature. In this study, the suitability of the suggested design rule by Gardner and Theofanous [20] for lean duplex stainless steel flexural members at elevated temperatures was examined. The design values calculated by the suggested EC3 in Gardner and Theofanous [20] at elevated temperatures is represented by $M_{G\&T,T}$. The mean value of $M_{FEA,T}/M_{G\&T,T}$ equal to 1.14 with a COV of 0.107 as well as the reliability index (β_0) of 2.7. The comparison of the numerical strengths, with the design values, is shown in Table 3 and Figure 7. It can be seen that the suggested design rule provided better predictions than the EC3 [19].

The classification limits and the effective width calculation in the European Code [19] were examined further in Huang and Young [7] using a large data pool of 180 lean duplex stainless steel flexural strengths at room temperature. Modified design rules by Huang and Young [7] were proposed and were shown to provide better predictions for lean duplex stainless steel flexural members at room temperature compared with the existing EC3 [19] and the design rule proposed by Gardner and Theofanous [20], as shown in Huang and Young [7]. In this study, the design rule modified by Huang and Young [7] was assessed for lean duplex stainless steel flexural members at elevated temperatures, by comparing the numerical moment strengths ($M_{FEA,T}$) with design values ($M^{\#}_{EC3,T}$). The mean value of $M_{FEA,T}/M^{\#}_{EC3,T}$ was equal to 1.14 with the corresponding COV of 0.105 as well as the reliability index (β_0) of 2.7, as shown in Table 3 and Figure 7. Therefore, the EC3 modified by Huang and Young [7] provided a slightly better prediction for lean duplex stainless steel flexural strength at elevated temperatures compared with the design rule suggested by Gardner and Theofanous [20].

4.4 Direct Strength Method

The direct strength method used in this study was based on Clause 1.2.2.1 of Appendix 1 in the North American Specification for the Design of Cold-Formed Steel Structural Members (AISI) [21]. Nominal flexural strength is determined by the minimum of the nominal flexural strength for lateral-torsional buckling (M_{ne}), local buckling (M_{nl}) and distortional buckling (M_{nd}). The lateral-torsional buckling and distortional buckling did not occur for SHS and RHS in this study. Flexural strength for local buckling (M_{nl}) is calculated by Eqs F3.2.1-1 and 3.2.1-2 in AISI [21] when the inelastic bending reserve is not considered. Alternatively, when the inelastic reserve local buckling strength is considered, Eq. F3.2.3-1 in AISI [21] is used for sections with first yield in compression. In this study, the nominal flexural strengths, calculated by the AISI [21] with and without considering the inelastic bending reserve, were represented by M_{DSM} and $M^{\wedge}_{DSM}$, respectively. The critical elastic local buckling moment (M_{crl}) of the cross-section was obtained from a rational elastic finite strip buckling analysis [22] with a 5 mm half-wave length interval.

The direct strength method (DSM) in AISI [21] was shown to provide conservative predictions for lean duplex stainless steel flexural members at room temperature and elevated temperatures, as shown in Huang and Young [7] and Table 3. The numerical strengths for lean duplex

stainless steel flexural members were compared with the design values calculated by the DSM with and without considering the inelastic bending reserve at elevated temperatures, represented by $M_{DSM,T}$ and $M^{\wedge}_{DSM,T}$, respectively. The mean values of numerical-to-design strengths for lean duplex stainless steel flexural members at elevated temperatures $M_{FEA,T}/M_{DSM,T}$ and $M_{FEA,T}/M^{\wedge}_{DSM,T}$ were 1.34 and 1.16 with the corresponding COVs of 0.179 and 0.107, respectively. The reliability indices (β_0) of $M_{FEA,T}/M_{DSM,T}$ and $M_{FEA,T}/M^{\wedge}_{DSM,}$ were 3.05 and 2.95. Both methods were considered to be reliable but conservative.

Modifications to the DSM were proposed for lean duplex stainless steel flexural members in Huang and Young [7]. The numerical flexural strengths at elevated temperatures in this study were also compared with the flexural strengths predicted by the modified DSM ($M^{\#}_{DSM,T}$), as shown in Table 3. It can be seen that the modified DSM provides accurate predictions for the lean duplex stainless steel flexural members at elevated temperatures with the mean value of $M_{FEA,T}/M^{\#}_{DSM,T}$ equal to 1.02 with COV of 0.090. The reliability index (β_0) was 2.51, which was greater than the target value of 2.5. The comparison of the numerical strengths, with the design values calculated by the existing and modified DSM, is shown in Table 3 and Figure 8.

4.5 Continuous Strength Method

The continuous strength method (CSM) proposed by Saliba and Gardner [9] was assessed for flexural members at elevated temperatures. The calculation procedure of CSM was the same as those described in Huang and Young [7]. The CSM does not apply to cross-sections where the slenderness ($\overline{\lambda}_p$) is larger than 0.748, because there is no significant benefit to be derived from strain hardening beyond this limit [9]. Therefore, the flexural strengths of 98 specimens that meet the requirement of the CSM are compared with the design values ($M_{CSM,T}$) calculated by the continuous strength method, as shown in Table 3. The material properties obtained from the tensile coupon tests at elevated temperatures were used in the calculation. The CSM was found to provide accurate predictions for the flexural members at elevated temperatures. The mean value of $M_{FEA,T}/M_{CSM,T}$ ratio was 1.02 with a COV of 0.081. The reliability index (β_0) was 2.35, which was considered not reliable at its current resistance factor (ϕ_0) of 0.91 and the load combination. However, the reliability index (β_1) of 2.54 was greater than the target value, when the resistance factor (ϕ_1) was calibrated to 0.90 and also using the load combination of

1.2DL+1.6LL as specified in the ASCE Specification, where DL was the dead load and LL was the live load.

5. Conclusions

The study reported here investigated the structural performance of lean duplex stainless steel flexural members at elevated temperatures. The flexural strengths obtained from the finite element analysis were compared with the design strengths calculated by the existing design rules. The design rules in ASCE [17] and AS/NZS [18] were found to provide quite conservative predictions for the cold-formed lean duplex stainless steel flexural members at elevated temperatures. Modifications to the inelastic reserve capacity approach have been proposed by Huang and Young [7] for flexural members at room temperature. Huang and Young [7] found that the modified design rules provide more accurate and less scattered predictions for the moment capacities at elevated temperatures. The EC3 [19] and the EC3 suggested by Gardner and Theofanous [20] provide less conservative predictions for the flexural members at elevated temperatures than the predictions for members at room temperature. The modified EC3 provides better predictions for flexural members at room temperature compared with those of the existing EC3 and the suggested EC3 by Gardner and Theofanous [20], while it provides similar predictions for the flexural members at elevated temperatures. The direct strength method in the AISI [21] provides quite conservative predictions for flexural members at elevated temperatures. A modified direct strength method was proposed by Huang and Young [7] for flexural members at room temperature, and this modified direct strength method was also used for flexural members at elevated temperatures. They found that the modified direct strength method also provides accurate and reliable predictions for flexural members at elevated temperatures. The continuous strength method was also shown to provide accurate predictions for flexural members at elevated temperatures, but not to be reliable when the existing resistance factor of 0.91 is used. Considering the accuracy, reliability and convenience of the various design rules, it is suggested to use the modified direct strength method for the design of cold-formed lean duplex stainless steel flexural members at elevated temperatures.

Acknowledgements

The research work described in this paper was supported by a grant from The University of Hong Kong under the seed funding program for basic research, and the Start-up Fund for Dr. Yuner Huang, sponsored by University of Edinburgh.

Notation

The following symbols are used in this paper:

B	overall width of cross-section of specimen
C_y	compression strain factor in American Specification and Australian/New Zealand Standard
c	flat width of specimen;
D	overall depth of cross-section of specimen
d_w	depth of the compressed portion of the web
f_y	yield strength (0.2% proof stress)
F_m	mean value of fabrication factor
$k_{FEA,T}$	curvature corresponding to the ultimate moment predicted by finite element analysis at elevated temperature
L	length of specimen
M_{crl}	critical elastic local buckling moment
$M_{CSM,T}$	unfactored design moment capacity predicted by the continuous strength method at elevated temperatures
$M_{DSM,T}$	unfactored design moment capacity predicted by the direct strength method at elevated temperatures
$M_{DSM,T}$	unfactored design moment capacity predicted by the direct strength method without considering the inelastic bending reserve at elevated temperatures
M_d	moment capacities predicted by design rules
M_{EC3}	unfactored design second-order elastic moment of beam-column for European Code at room temperature
$M_{EC3,T}$	unfactored design second-order elastic moment of beam-column for European Code at elevated temperatures
$M_{FEA,T}$	ultimate moment predicted by finite element analysis at elevated temperatures
$M_{G\&T,T}$	unfactored design moment capacity predicted by the modified European Code by Gardner and Theofanous at elevated temperatures
$M_{inelastic,T}$	unfactored design moment capacity predicted by the approach by inelastic reserve capacity in American Specification and Australian/New Zealand Standard at elevated temperatures

M_m mean value of material factor

M_{nd} nominal flexural strength for distortional buckling in direct strength method

M_{ne} nominal flexural strength for lateral-torsional buckling in direct strength method

M_{nl} nominal flexural strength for local buckling in direct strength method

M_u experimental and numerical ultimate moments

M_y yield moment

$M_{yielding,T}$ unfactored design moment capacity predicted by the approach by initiation of yielding in American Specification and Australian/New Zealand Standard at elevated temperatures

$M^{\#}_{DSM,T}$ unfactored design moment capacity predicted by the modified direct strength method at elevated temperatures

$M^{\#}_{EC3,T}$ unfactored design moment capacity predicted by the modified European Code at elevated temperatures

$M^{\#}_{inelastic,T}$ unfactored design moment capacity predicted by the modified approach by inelastic reserve capacity at elevated temperatures

$M^{\wedge}_{DSM,T}$ unfactored design moment capacity predicted by the direct strength method with considering the inelastic bending reserve at elevated temperatures

P_m mean value of tested-to-predicted load ratio

S_e effective section modulus

t thickness of specimen

T temperature in ºC;

V_F coefficient of variation of fabrication factor

V_m coefficient of variation of material factor

V_p coefficient of variation of test and finite element to design predictions

β_0 reliability index

β_1 reliability index

ε material factor

ϕ_o resistance factor

ϕ_1 resistance factor

λ_l non-dimensional slenderness to determine P_{nl}

$\overline{\lambda}_p$ element slenderness

References

[1] Yrjola P. *Stainless steel hollow sections handbook.* Finnish Constructional Steelwork Association, Finland, 2008.

[2] Huang, Y., and Young, B. (2012). "Material properties of cold-formed lean duplex stainless steel sections." *Thin-Walled Structures*, 54: 72-81.

[3] Theofanous, M., and Gardner, L. (2009). "Testing and numerical modelling of lean duplex stainless steel hollow section columns." *Engineering Structures*, 31(12): 3047-3058.

[4] Huang, Y., and Young, B. (2013). "Tests of pin-ended cold-formed lean duplex stainless steel columns." *Journal of Constructional Steel Research*, 82: 203-215.

[5] Huang, Y., and Young, B. (2014). "Structural performance of cold-formed lean duplex stainless steel columns." *Thin-Walled Structures*, 83: 59 – 69.

[6] Anbarasu, M., and Ashraf, M. (2016). "Behaviour and design of cold-formed lean duplex stainless steel lipped channel columns." *Thin-Walled Structures*, 104: 106 – 115.

[7] Huang, Y., and Young, B. (2013). "Experimental and numerical investigation of cold-formed lean duplex stainless steel flexural members." *Thin-Walled Structures*, 73: 216-228.

[8] Theofanous, M., and Gardner, L. (2010). "Experimental and numerical studies of lean duplex stainless steel beams." *Journal of Constructional Steel Research*, 66(6): 816-825.

[9] Saliba, N., and Gardner, L. (2013). "Cross-section stability of lean duplex stainless steel welded I-sections." *Journal of Constructional Steel Research*, 80: 1-14.

[10] Sonu, J.K., and Singh, K.D. (2017). "Shear characteristics of lean duplex stainless steel (LDSS) rectangular hollow beams." *Structures*, 10: 13 – 29.

[11] Huang, Y., and Young, B. (2014). "Experimental investigation of cold-formed lean duplex stainless steel beam-columns." *Thin-Walled Structures*, 76: 105 – 117.

[12] Huang, Y., and Young, B. (2015). "Design of cold-formed lean duplex stainless steel members in combined compression and bending." *Journal of Structural Engineering, ASCE*, 141(5): 04014138.

[13] Huang, Y., and Young, B. (2013). "Stress-strain relationship of cold-formed lean duplex stainless steel at elevated temperatures." *Journal of Constructional Steel Research*, 92: 103 – 113.

[14] Gardner, L., Insausti, A., Ng, K.T., and Ashraf, M. (2010). "Elevated temperature material properties of stainless steel alloys." *Journal of Constructional Steel Research*, 66(5): 634-647.

[15] Outokumpu. (2008). Anisothermal tests on stainless steel grades. Confidential Outokumpu report.

[16] ABAQUS. (2011). *Standard User's Manual*. Version 6.11. Dassault Systemes Simulia Corp., USA.

[17] ASCE. (2002). *Specification for the design of cold-formed stainless steel structural members*. SEI/ASCE 8-02. American Society of Civil Engineers. Reston, Virginia, USA.

[18] AS/NZS. (2001). *Cold-formed stainless steel structures*. AS/NZS 4673, Australian/New Zealand Standard, Standards Australia. Sydney, Australia.

[19] EC3. (2006b). *Eurocode 3: Design of steel structures – Part 1.4: General rules – Supplementary rules for stainless steels*. ENV 1993-1-4, CEN. European Committee for Standardization, Brussels.

[20] Gardner, L., and Theofanous, M. (2008). "Discrete and continuous treatment of local buckling in stainless steel elements." *Journal of Constructional Steel Research*, 64(11): 1207-1216.

[21] AISI S100. (2016). *North American Specification for the design of cold-formed steel structural members.* AISI S100-16, North American Cold-formed Steel Specification. American Iron and Steel Institute, Washington D.C., USA.

[22] Papangelis, J.P., and Hancock, G.J. (1995). "Computer analysis of thin-walled structural members." *Computers & Structures*, 56(1): 157–176.

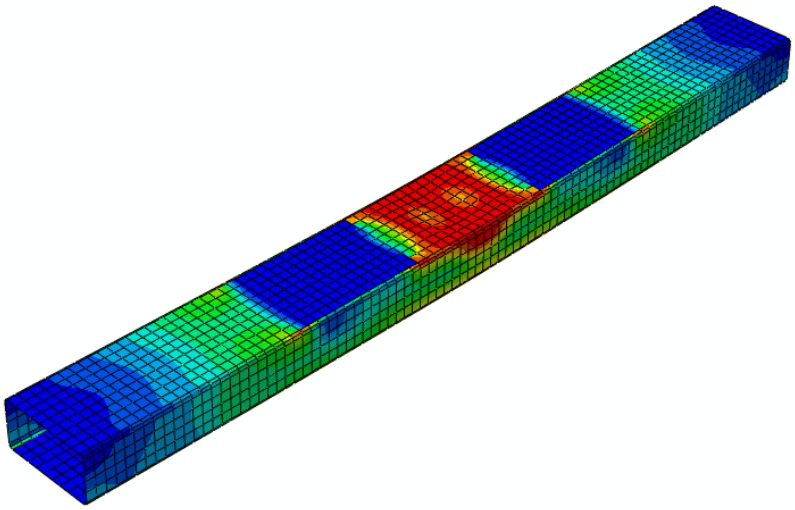

Figure 1: Finite element model of specimen 50×100×2L900T700 in parametric study

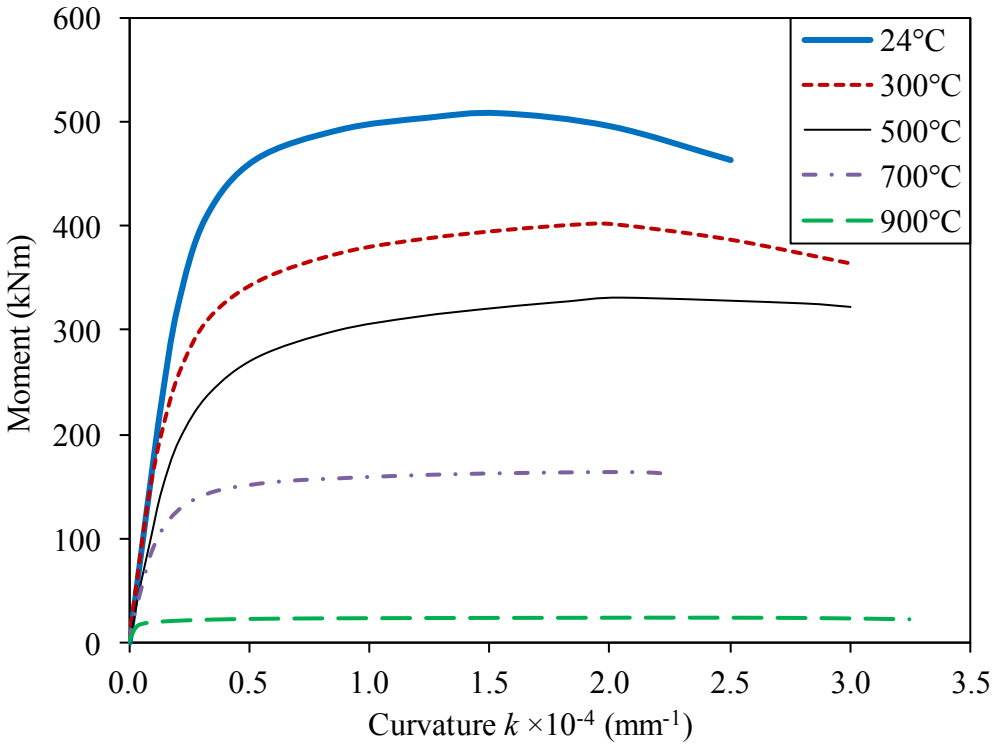

Figure 2: Moment-curvature curves obtained from FEA for specimen 300×100×10L2100 at elevated temperatures

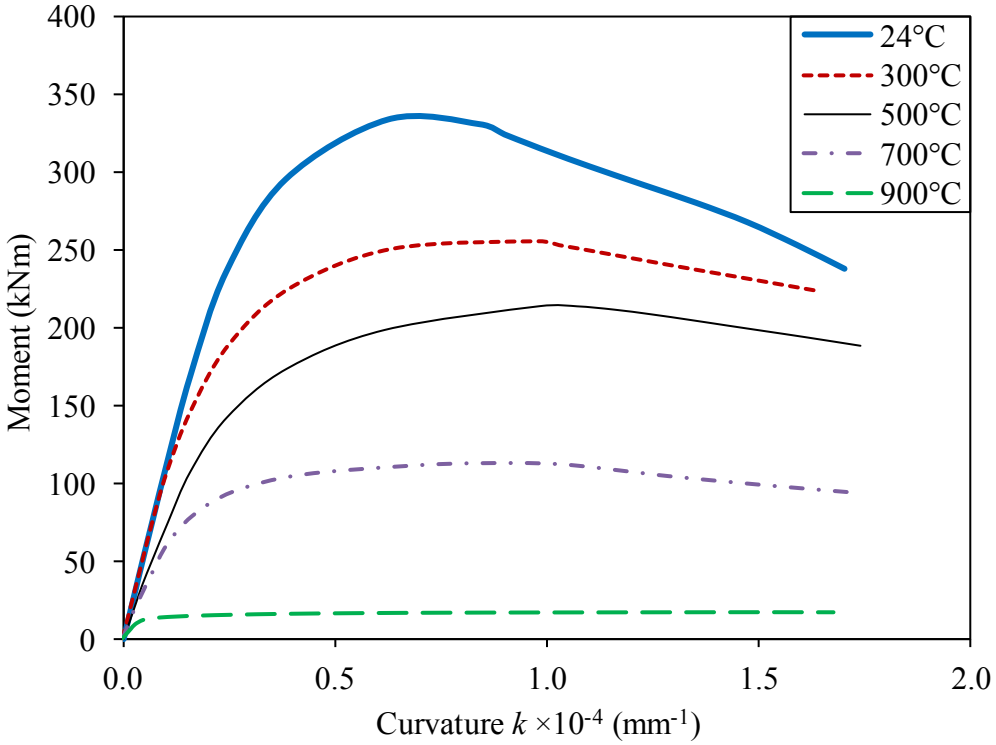

Figure 3: Moment-curvature curves obtained from FEA for specimen 300×100×7L2100 at elevated temperatures

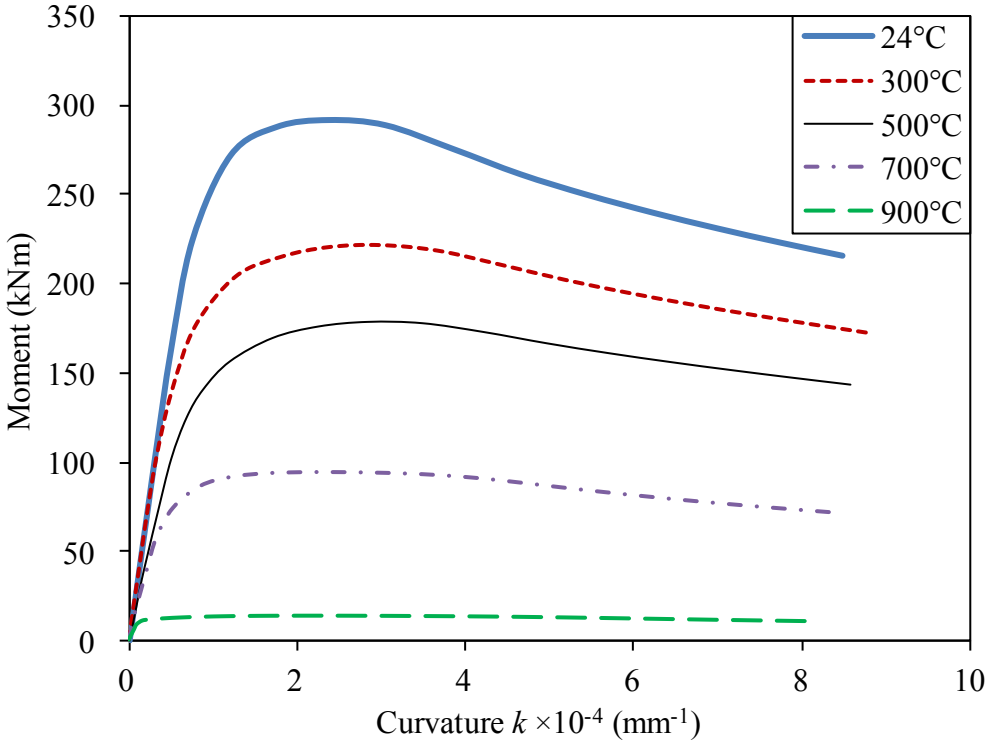

Figure 4: Moment-curvature curves obtained from FEA for specimen 100×300×15L1500 at elevated temperatures

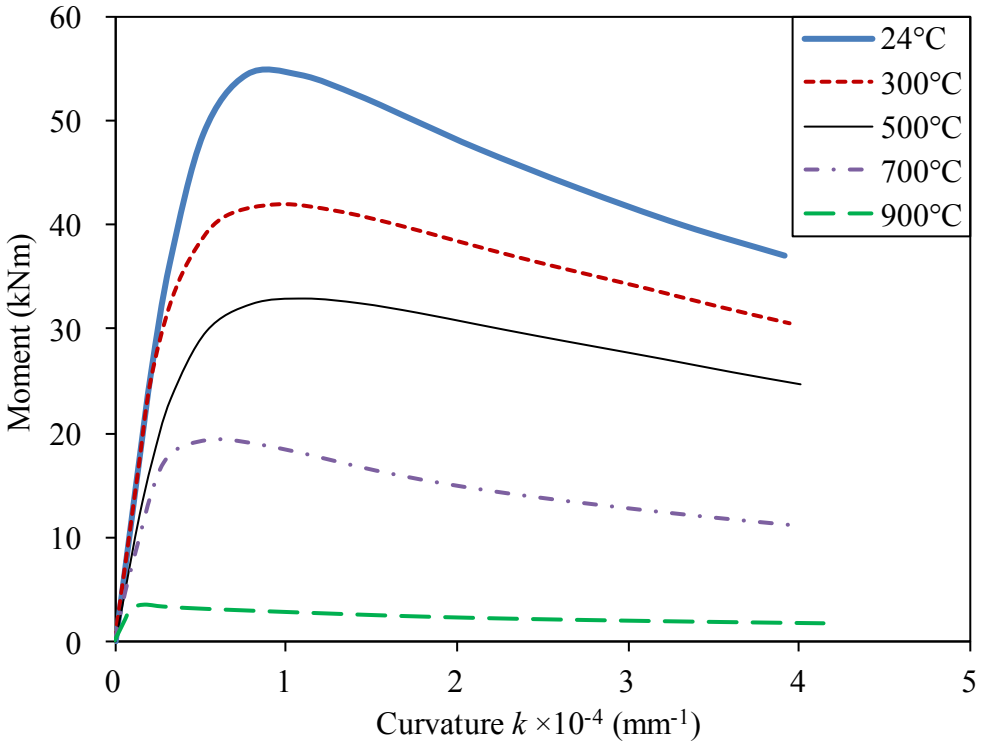

Figure 5: Moment-curvature curves obtained from FEA for specimen 100×300×4L1500 at elevated temperatures

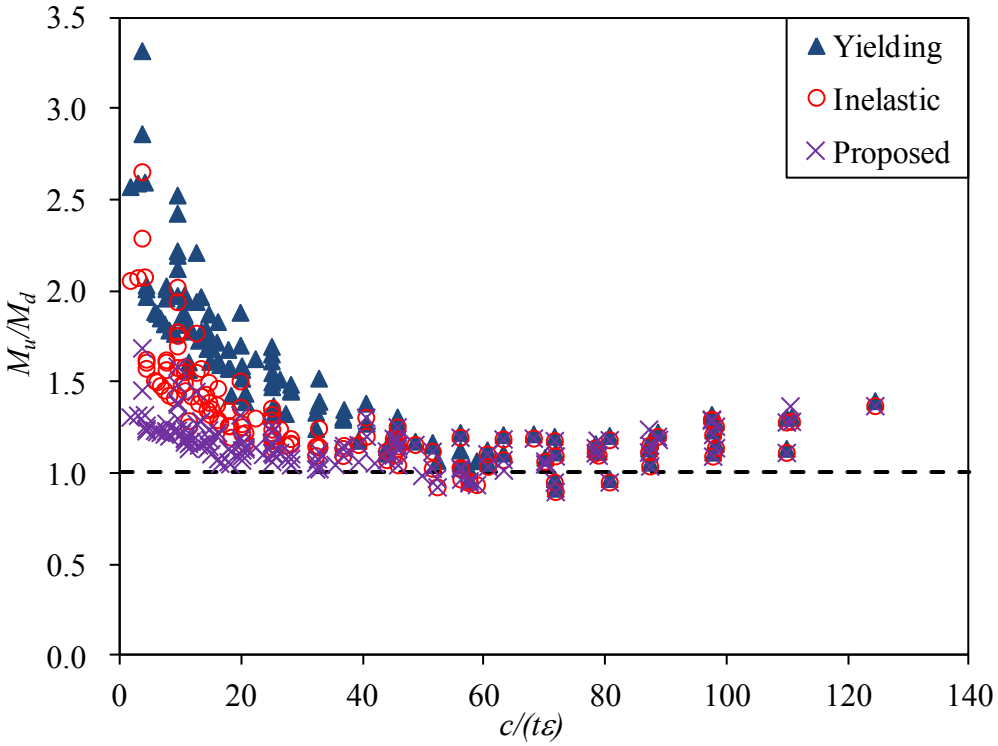

Figure 6: Comparison of numerical results with design strengths by ASCE and AS/NZS at elevated temperatures

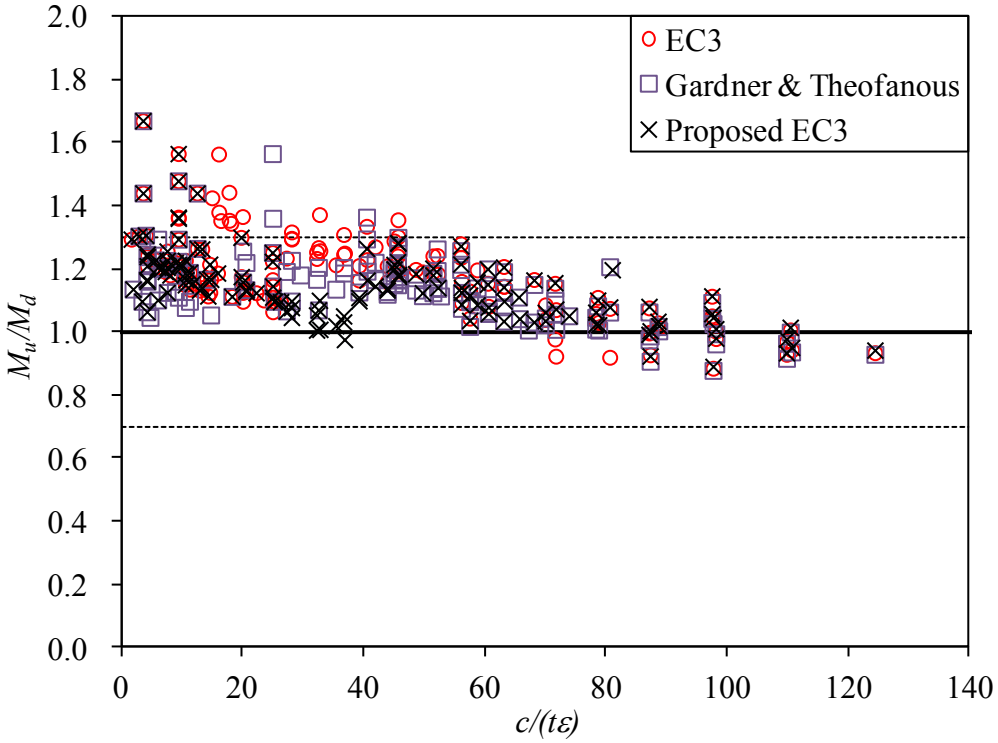

Figure 7: Comparison of numerical results with design strengths by EC3 at elevated temperatures

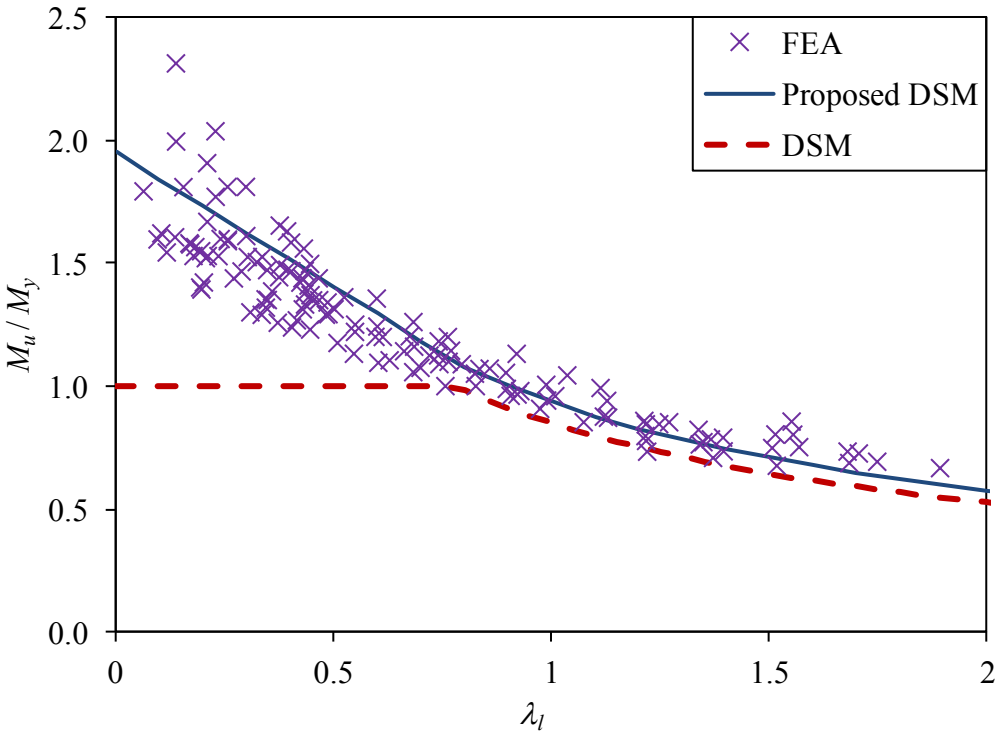

Figure 8: Comparison of numerical results with design strengths by DSM at elevated temperatures

T (ºC)	E_o (GPa)	f_y (MPa)	f_u (MPa)	ε_u (%)
24	199.0	682.4	828.1	21.5
100	195.0	641.5	803.3	19.4
200	175.1	566.4	728.7	18.7
300	187.1	511.8	695.6	16.6
400	159.2	443.6	687.3	18.9
500	139.3	375.3	596.2	17.4
600	125.4	266.1	347.8	10.8
700	121.4	211.5	248.4	10.3
800	65.7	95.5	115.9	3.2
900	55.7	27.3	33.1	2.6

Table 1: Material properties of the specimens at high temperatures [12]

Specimen ($D\times B\times t$)	$M_{FEA,T}$ (kNm)	$k_{FEA,T}\times 10^{-4}$ (mm^{-1})
300×300×25L3000T24	2138.0	3.91
300×300×25L3000T300	1729.5	4.34
300×300×25L3000T500	1448.7	4.89
300×300×25L3000T700	682.9	3.46
300×300×25L3000T900	99.6	2.35
300×300×15L3000T24	1319.1	0.89

300×300×15L3000T300	1027.1	1.39
300×300×15L3000T500	825.6	1.37
300×300×15L3000T700	428.7	1.19
300×300×15L3000T900	63.2	1.51
300×300×10L3000T24	821.4	0.44
300×300×10L3000T300	621.8	0.41
300×300×10L3000T500	496.9	0.49
300×300×10L3000T700	276.4	0.43
300×300×10L3000T900	41.3	0.35
300×300×7L3000T24	519.9	0.57
300×300×7L3000T300	368.1	0.45
300×300×7L3000T500	289.2	0.46
300×300×7L3000T700	175.7	0.27
300×300×7L3000T900	28.5	0.27
300×300×5L3000T24	289.4	0.27
300×300×5L3000T300	211.1	0.34
300×300×5L3000T500	167.0	0.32
300×300×5L3000T700	103.8	0.22
300×300×5L3000T900	18.8	0.14
100×50×8L900T24	53.0	29.06
100×50×8L900T300	43.6	27.47
100×50×8L900T500	37.2	28.79
100×50×8L900T700	16.3	23.44
100×50×8L900T900	2.3	8.30
100×50×5L900T24	34.7	17.06
100×50×5L900T300	28.7	18.24
100×50×5L900T500	24.3	18.53
100×50×5L900T700	10.9	15.64
100×50×5L900T900	1.6	6.42
100×50×3L900T24	20.6	3.71
100×50×3L900T300	16.0	4.24
100×50×3L900T500	13.0	4.24
100×50×3L900T700	6.7	4.99
100×50×3L900T900	1.0	6.02
100×50×2L900T24	12.4	1.28
100×50×2L900T300	9.5	1.75
100×50×2L900T500	7.6	1.70
100×50×2L900T700	4.3	1.59
100×50×2L900T900	0.7	2.79
100×50×1L900T24	3.8	0.66
100×50×1L900T300	3.0	0.72
100×50×1L900T500	2.3	0.86
100×50×1L900T700	1.5	0.39
100×50×1L900T900	0.3	0.47
50×100×5L900T24	18.8	5.34
50×100×5L900T300	14.4	6.74
50×100×5L900T500	11.7	7.26
50×100×5L900T700	6.0	5.79
50×100×5L900T900	0.9	5.39

50×100×3L900T24	10.6	2.02
50×100×3L900T300	8.1	2.83
50×100×3L900T500	6.4	2.74
50×100×3L900T700	3.7	2.29
50×100×3L900T900	0.6	2.98
50×100×2.5L900T24	8.2	1.97
50×100×2.5L900T300	6.3	1.91
50×100×2.5L900T500	4.9	2.68
50×100×2.5L900T700	3.0	1.58
50×100×2.5L900T900	0.5	2.03
50×100×2L900T24	6.0	1.93
50×100×2L900T300	4.6	2.65
50×100×2L900T500	3.6	2.84
50×100×2L900T700	2.1	1.55
50×100×2L900T900	0.4	1.32
50×100×1.5L900T24	4.0	0.99
50×100×1.5L900T300	2.8	0.42
50×100×1.5L900T500	2.4	1.11
50×100×1.5L900T700	1.4	0.89
50×100×1.5L900T900	0.3	1.78
300×100×10L2100T24	508.9	1.54
300×100×10L2100T300	400.9	2.02
300×100×10L2100T500	331.5	2.05
300×100×10L2100T700	164.3	1.86
300×100×10L2100T900	23.7	1.28
300×100×8L2100T24	396.0	0.72
300×100×8L2100T300	310.4	1.01
300×100×8L2100T500	252.9	1.05
300×100×8L2100T700	130.9	1.10
300×100×8L2100T900	19.4	1.59
300×100×7.5L2100T24	356.2	0.61
300×100×7.5L2100T300	289.2	1.14
300×100×7.5L2100T500	229.6	0.99
300×100×7.5L2100T700	122.4	1.19
300×100×7.5L2100T900	18.3	2.05
300×100×7L2100T24	333.9	0.62
300×100×7L2100T300	255.8	0.98
300×100×7L2100T500	213.3	0.98
300×100×7L2100T700	112.9	0.84
300×100×7L2100T900	17.1	1.52
300×100×6.5L2100T24	318.3	0.77
300×100×6.5L2100T300	235.5	0.86
300×100×6.5L2100T500	184.6	0.61
300×100×6.5L2100T700	103.9	0.69
300×100×6.5L2100T900	15.8	1.16
100×300×15L1500T24	291.4	2.37
100×300×15L1500T300	221.2	3.00
100×300×15L1500T500	178.3	2.83
100×300×15L1500T700	94.1	2.44

100×300×15L1500T900	14.0	2.24
100×300×8L1500T24	142.7	0.86
100×300×8L1500T300	108.7	1.17
100×300×8L1500T500	84.0	0.93
100×300×8L1500T700	51.2	0.74
100×300×8L1500T900	8.1	1.38
100×300×5.5L1500T24	84.3	1.05
100×300×5.5L1500T300	64.0	0.74
100×300×5.5L1500T500	50.7	0.72
100×300×5.5L1500T700	30.1	0.40
100×300×5.5L1500T900	5.4	0.33
100×300×5L1500T24	74.3	1.08
100×300×5L1500T300	56.5	0.93
100×300×5L1500T500	44.8	1.08
100×300×5L1500T700	26.1	0.60
100×300×5L1500T900	4.8	0.39
100×300×4L1500T24	54.5	0.77
100×300×4L1500T300	41.9	0.96
100×300×4L1500T500	32.9	1.11
100×300×4L1500T700	19.4	0.60
100×300×4L1500T900	3.6	0.19

Table 2: Parametric study results at elevated temperatures

	ASCE			AS/NZS			EC3			DSM			CSM
	$\frac{M_{FEA,T}}{M_{yielding,T}}$	$\frac{M_{FEA,T}}{M_{inelastic,T}}$	$\frac{M_{FEA,T}}{M^{\#}_{inelastic,T}}$	$\frac{M_{FEA,T}}{M_{yielding,T}}$	$\frac{M_{FEA,T}}{M_{inelastic,T}}$	$\frac{M_{FEA,T}}{M^{\#}_{inelastic,T}}$	$\frac{M_{FEA,T}}{M_{EC3,T}}$	$\frac{M_{FEA,T}}{M_{G\&T,T}}$	$\frac{M_{FEA,T}}{M^{\#}_{EC3,T}}$	$\frac{M_{FEA,T}}{M_{DSM,T}}$	$\frac{M_{u}}{\hat{M}_{DSM,T}}$	$\frac{M_{FEA,T}}{M^{\#}_{DSM,T}}$	$\frac{M_{FEA,T}}{M_{CSM,T}}$
# of data	125	111	125	125	111	125	125	125	125	125	125	125	98
Mean (P_m)	1.51	1.30	1.16	1.51	1.30	1.16	1.19	1.14	1.14	1.34	1.16	1.02	1.02
COV (V_p)	0.277	0.213	0.105	0.277	0.213	0.105	0.112	0.107	0.105	0.179	0.107	0.090	0.081
Resistance factor ($\nearrow_0$)	0.90	0.90	0.90	0.90	0.90	0.90	0.91	0.91	0.91	0.90	0.90	0.90	0.91
Reliability index (β_0)	2.80	2.74	2.97	2.65	2.57	2.75	2.82	2.70	2.70	3.05	2.95	2.51	2.35
Resistance factor ($\nearrow_1$)	0.90	0.90	0.90	0.90	0.90	0.90	0.90	0.90	0.90	0.90	0.90	0.90	0.90
Reliability index (β_1)	2.80	2.74	2.97	2.80	2.74	2.97	3.01	2.89	2.89	3.05	2.95	2.51	2.54

[#] Modified design rules

Table 3: Comparison of numerical results with design moment capacities at elevated temperatures